Optics Letters

High speed and high resolution interrogation of a fiber Bragg grating sensor based on microwave photonic filtering and chirped microwave pulse compression

Ou Xu,[1,2] Jiejun Zhang,[1] and Jianping Yao[1,*]

[1]*Microwave Photonic Research Laboratory, School of Electrical Engineering and Computer Science, University of Ottawa, Ontario K1N6N5, Canada*
[2]*School of Information Engineering, Guangdong University of Technology, Guangzhou, 510006, China*
Corresponding author: jpyao@eecs.uottawa.ca

High speed and high resolution interrogation of a fiber Bragg grating (FBG) sensor based on microwave photonic filtering and chirped microwave pulse compression is proposed and experimentally demonstrated. In the proposed sensor, a broadband linearly chirped microwave waveform (LCMW) is applied to a single-passband microwave photonic filter (MPF) which is implemented based on phase modulation and phase modulation to intensity modulation conversion using a phase modulator (PM) and a phase-shifted FBG (PS-FBG). Since the center frequency of the MPF is a function of the central wavelength of the PS-FBG, when the PS-FBG experiences a strain or temperature change, the wavelength is shifted, which leads to the change in the center frequency of the MPF. At the output of the MPF, a filtered chirped waveform with the center frequency corresponding to the applied strain or temperature is obtained. By compressing the filtered LCMW in a digital signal processor, the resolution is improved. The proposed interrogation technique is experimentally demonstrated. The experimental results show that interrogation sensitivity and resolution as high as 1.25 ns/µε and 0.8 µε are achieved. © 2016 Optical Society of America

Fiber optic sensors with advantages, such as immunity to electromagnetic interference (EMI) and remote and distributed sensing, can find important applications in aerospace, civil engineering, electric power engineering, petrochemical industry, medical care, and homeland security [1]. Fiber grating-based sensors are wavelength-encoded, and have merits, such as high stability, reliability, and advanced multiplexing capabilities [2]. For practical applications, high speed and accurate interrogations for wavelength-encoded sensing is important, and numerous techniques have been proposed. In general, a fiber grating-based sensor can be interrogated using an optical spectrum analyzer (OSA), an optical edge filter [3], a Fabry–Perot filter [4], or an unbalanced Mach–Zehnder interferometer [5]. However, the performance of these interrogation techniques is limited by either the interrogation speed (lower than kHz) or resolution (generally poorer than 1 pm) [6]. For high speed sensing applications, such as impact damage detection and vibration sensing, high speed and high resolution interrogation is necessary.

Microwave photonics (MWP), a field that studies the generation, processing, control, and distribution of microwave signals by means of photonics [7], has been recently investigated for the implementation of high speed and high resolution fiber optic sensors [8]. The fundamental concept of using MWP to perform fiber optic sensing is to convert the wavelength change in the optical domain to the frequency change of a microwave signal in the electrical domain. Since the frequency of a microwave signal can be measured at a high speed and high resolution using a digital signal processor (DSP), an MWP-based fiber optic sensor can operate at high speeds and high resolutions. For example, a linearly chirped fiber Bragg grating (LCFBG) sensor based on MWP was proposed and demonstrated recently. Based on spectral shaping and wavelength-to-time (SS-WTT) mapping [9], a linearly chirped microwave waveform (LCMW) with a center frequency that is a function of the wavelength change of the LCFBG was generated. The resolution was improved by compressing the chirped waveform by correlation in a DSP [10]. In Ref. [11], a transverse load sensor based on a dual-frequency optoelectronic oscillator (OEO) was proposed, in which the wavelength change was converted to the frequency change of the generated microwave signal. For distributed sensing, the interrogation of a long weak FBG sensor using a microwave photonic filter (MPF) was proposed [12], where the weak FBG was used as a distributed sensor with multiple hot spots on the FBG to change the tap coefficients of the MPF. By monitoring the spectral response of the MPF, the sensing information was estimated. Recently, a simple approach

to interrogate an LCFBG sensor by reflecting a linearly chirped optical waveform using two LCFBGs with one as a sensor and the other as a reference was demonstrated [13]. However, the approach reported in [10] requires the use of a mode-locked laser source, which makes the system complicated and costly [10]. The OEO-based approach is simple, but the stability is an issue since the OEO loop must be very short to avoid mode hopping [11]. The distributed sensor using long weak FBG requires the use of an electrical network analyzer to monitor the spectral response of the MPF, which makes the interrogation very slow and costly [12]. The approach reported in [13] can have an ultra-fast interrogation. The only limitation is the difficulty in generating a linearly chirped optical waveform which may make the system complicated.

In this Letter, a novel technique to interrogate an FBG sensor based on microwave photonic filtering and chirped microwave pulse compression at a high speed and high resolution is proposed and experimentally demonstrated. In the proposed interrogation system, a broadband LCMW is applied to a single-passband MPF, which is implemented based on phase modulation and phase modulation to intensity modulation (PM-IM) conversion using a phase modulator (PM) and a phase-shifted FBG (PS-FBG) [14]. Since the center frequency of the MPF is a function of the central wavelength of the notch of the PS-FBG, when the PS-FBG experiences a strain or temperature change, the wavelength is shifted, which leads to the change in the center frequency of the MPF. At the output of the MPF, a filtered LCMW with the center frequency corresponding to the applied strain or temperature is obtained. By compressing the filtered LCMW based on correlation in a DSP, the resolution is improved. The proposed technique is experimentally demonstrated. An interrogation sensitivity and resolution as high as 1.25 ns/µε and 0.8 µε are achieved.

Figure 1 shows the configuration of the proposed PS-FBG sensor. The entire system is a MPF followed by a DSP. The MPF (in the dotted line in Fig. 1) is implemented using a PM and a PS-FBG, by transferring the notch of the PS-FBG to the passband of a MPF based on phase modulation and PM-IM conversion. As observed, in Fig. 1, a light wave from a tunable laser source (TLS) is sent to a PM via a polarization controller (PC). The phase-modulated signal at the output of the PM is sent to the PS-FBG. By filtering out one sideband of the phase-modulated signal by the notch, PM-IM conversion is performed. By applying the intensity-modulated signal at a PD, a MPF having a passband with the center frequency determined by the wavelength difference between the light wave and the

Fig. 1. Schematic diagram of the proposed FBG sensor. TLS, tunable laser source; AWG, arbitrary waveform generator; PM, phase modulator; PD, photodetector; VNA, vector network analyzer; OSC, oscilloscope; DSP, digital signal processor.

notch is realized. For sensor application, here we apply a broadband LCMW to the input of the MPF. At the output of the MPF, a filtered LCMW with the center frequency determined by the center frequency of the passband of the MPF is obtained. To improve the resolution, the filtered LCMW is compressed by correlating it with the waveform applied to the input of the MPF, which is done in a DSP.

The key to implement the proposed interrogation system is to have a MPF, with a center frequency of the passband as a function of the wavelength change of the notch of the PS-FBG. If the optical carrier frequency or wavelength is f_C or λ_C and the center frequency or wavelength of the notch is $f_{\text{PS-FBG}}$ or $\lambda_{\text{PS-FBG}}$, the center frequency of the passband of the MPF is the difference between the two frequencies, which is given by

$$f_{\text{MPF}} = f_{\text{PS-FBG}} - f_C \approx \frac{c}{n} \cdot \left(\frac{\lambda_C - \lambda_{\text{PS-FBG}}}{\lambda_C^2} \right), \quad (1)$$

where f_{MPF} is the frequency of the passband of the MPF, c is the velocity of light in vacuum, and n is the effective refractive index of the fiber. When the PS-FBG experiences a strain, the central wavelength of the notch will shift due to the variation of the grating pitch. As a result, the central wavelength of the passband of the MPF will shift. Thus, we have the relationship between the strain and the wavelength change, given by

$$\Delta\lambda_{\text{PS-FBG}} = \lambda_{\text{PS-FBG}} \cdot (1 - P_e)\Delta\epsilon, \quad (2)$$

where P_e is the photo-elastic coefficient of the fiber. The corresponding frequency change of the passband of the MPF is

$$\Delta f_{\text{MPF}} = -\frac{c}{n\lambda_C^2} \cdot \lambda_{\text{PS-FBG}} \cdot (1 - P_e)\Delta\epsilon. \quad (3)$$

As observed, the frequency change is linearly proportional to the strain applied to the PS-FBG. If a broadband LCMW is applied to the input of the MPF, only the portion of the spectrum of the LCMW that falls in the passband will be obtained. By monitoring the center frequency of the filtered LCMW, the strain is measured.

Mathematically, a broadband LCMW can be expressed as [10]

$$s(t) = \text{rect}\left(\frac{t}{T}\right) \cdot \exp(jk\pi t^2), \quad (4)$$

where k is the chirp rate, $\text{rect}(t/T)$ is a rectangular window, and T is the temporal duration of the waveform.
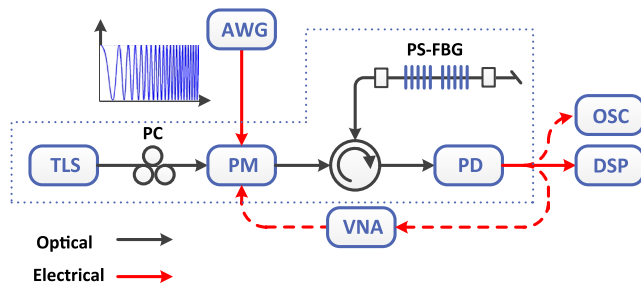
When the broadband chirped waveform is applied to the input of the MPF, we have the output signal, given by

$$H_{\text{output}}(f) = S(f) \cdot H_{\text{MPF}}(f), \quad (5)$$

$$H_{\text{MPF}}(f) = \frac{\pi^2 R^2}{V_\pi^2}[1 - R(f_c + f)]^2, \quad (6)$$

where $S(f)$ is the Fourier transform of $s(t)$, $H_{\text{MPF}}(f)$ is the frequency response of the MPF [14], which is a narrow passband filter with a center frequency of f_{MPF}, R is the photo-responsivity of the PD, V_π is the half-wave voltage of the PM, and $R(f)$ represents the reflection spectral profile of the PS-FBG. The peak of the pass band of the MPF appears when $R(f_c + f) = 0$, which means that the central frequency of the peak, f_{MPF}, satisfies $f_C + f_{\text{MPF}} = f_{\text{PS-FBG}}$.
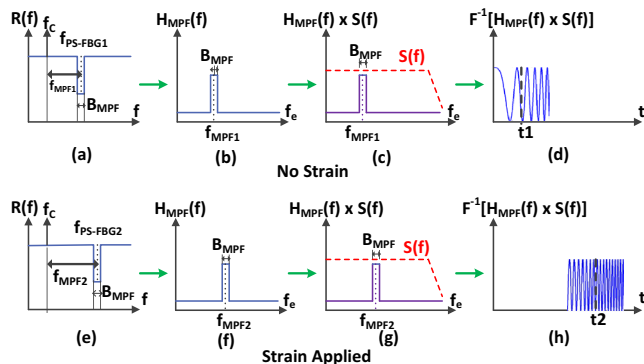
Figure 2 illustrates the working principle of the proposed sensor. As observed, the PS-FBG has a notch with a center

frequency of $f_{PS-FBG1} = f_C + f_{MPF1}$ when no strain is applied, as shown in Fig. 2(a). Due to the PM-IM modulation conversion in the PS-FBG, a MPF with a center frequency at f_{MPF1} is produced, as shown in Fig. 2(b). The spectrum of a broadband LCMW applied to the input of the MPF is shown in Fig. 2(c). The spectral components corresponding to the passband of the MPF will be transmitted to the output. The temporal waveform of the filtered broadband waveform is shown in Fig. 2(d). As observed, the waveform is chirped. When a strain is applied to the PS-FBG, the central frequency of the notch of the PS-FBG and that of the MPF will be both shifted, as shown in Figs. 2(e) and 2(f). The center frequency of the MPF is shifted to a new frequency, f_{MPF2}. The spectral components of the broadband microwave waveform corresponding to the new passband of the MPF will be transmitted to the output, as shown in Fig. 2(g). The temporal waveform of the filtered broadband waveform is shown in Fig. 2(h). Again, the waveform is linearly chirped, but the center frequency is shifted to a higher frequency. By measuring the center frequency in the microwave domain using a DSP, the strain applied to the PS-FBG can be measured. Since the spectrum width of the filtered LCMW is wide, the resolution is still low. To increase the resolution, the filtered LCMW can be compressed based on correlation between the filtered waveform and the input waveform. A significantly compressed pulse would be produced. By measuring the position of the compressed pulse, a high resolution interrogation of the strain can be realized.

An experiment based on the setup shown in Fig. 1 to verify the operation of the proposed PS-FBG interrogation system is performed. The key device in the MPF is the PS-FBG, which is fabricated using a uniform phase mask by scanning a UV beam along the axial direction of a hydrogen-loaded optical fiber. At the center of the grating, a phase shift is introduced by moving the phase mask to create a narrow notch in the reflection spectrum. The reflection and transmission spectra of the PS-FBG are measured using an optical vector analyzer (OVA, Luna Technologies) and shown in Fig. 3(a). A narrow notch at 1546.615 nm is observed. The total reflection bandwidth of the PS-FBG is about 0.55 nm and the 3-dB bandwidth of the notch is about 200 MHz. To have a wider frequency tunable range of the MPF, the notch is placed away
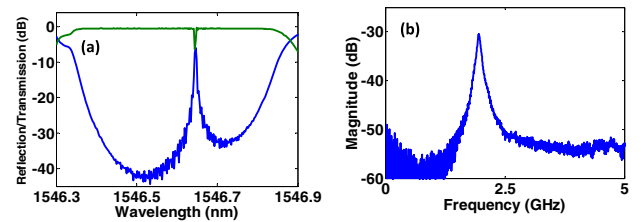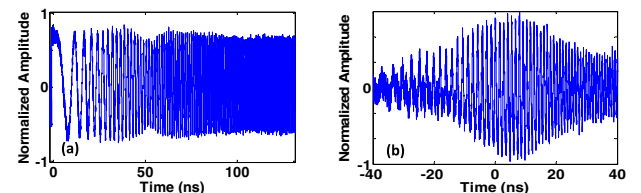

Fig. 3. (a) Measured reflection (green line) and transmission (blue line) spectra of the PS-FBG. (b) Measured frequency response magnitude of the MPF $|H_{MPF}(f)|^2$ by a microwave VNA.

from the center of the reflection spectrum, which is done by making a phase shift smaller than π.

The fabricated PS-FBG is incorporated into the proposed interrogation system. We first measure the spectral response of the MPF, which is done with a vector network analyzer (VNA, Agilent E8364A) by scanning the frequency of a microwave signal applied to the input of the MPF. In the measurement, the scanning frequency is from 45 MHz to 10 GHz. The highest frequency is determined by the bandwidth of the PM and the PD. The wavelength of the optical carrier is set to a value that is less than the center wavelength of the notch. Since the upper sideband will fall in the notch of the PS-FBG, the central frequency of the MPF is equal to the frequency difference between the frequency of the optical carrier and the center frequency of the notch, as illustrated in Figs. 2(a) and 2(e). Figure 3(b) shows the measured frequency response of the MPF.

A broadband LCMW is then applied to the input of the MPF. In the experiment, the broadband LCMW is generated by an arbitrary waveform generator (AWG, Keysight M9505A). Figure 4(a) shows the temporal waveform of the broadband LCMW measured by a real time oscilloscope (Keysight, DSO-Z 504A). The peak-to-peak voltage of the broadband waveform is about 1 V. The temporal duration of the waveform is 1 μs, and the chirp rate of the waveforms is 0.0127 GHz/ns. To clearly display the chirped waveform, Fig. 4(a) only presents part of the measured temporal waveform. Figure 4(b) shows the temporal waveform of the filtered chirped waveform. In order to more clearly demonstrate the chirped waveform, the central frequency of the MPF is set to a lower frequency, less than 1 GHz, by adjusting the carrier wavelength of the TLS. When a strain is applied to the PS-FBG, the center frequency of the filtered chirped waveform will be shifted to a higher frequency. Thus, the sensing information is coded in the output waveform as a center frequency change and temporal location.

Figure 5(a) shows five superimposed frequency responses of the MPF corresponding to five strains of 150 με, 175 με, 200 με, 225 με, and 250 με applied to the PS-FBG.

Fig. 2. Illustration of the operation of the interrogation system. (a) PS-FBG notch with no strain applied. (b) MPF spectral response with no strain. (c) Spectrum of the filtered signal. (d) Temporal waveform of the filtered signal. (e) PS-FBG notch with strain applied. (f) MPF spectral response with strain applied. (g) Spectrum of the filtered signal. (h) Temporal waveform of the filtered signal.

Fig. 4. (a) Broadband LCMW generated by an AWG. (b) Temporal waveform at the output of the MPF measured by an oscilloscope.
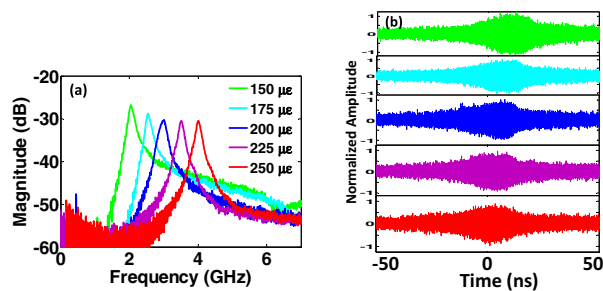
Fig. 5. (a) Five superimposed frequency responses of the MPF corresponding to five strains applied to the PS-FBG. (b) Corresponding five output chirped microwave waveforms with different temporal locations.
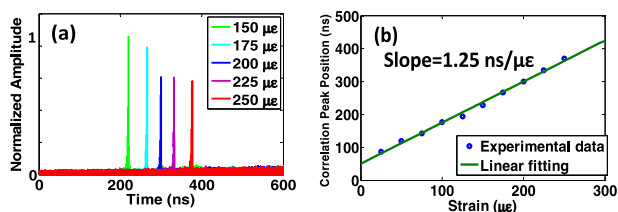
Fig. 6. (a) Correlation outputs of the five filtered LCMW. (b) Correlation peak position vs. applied strain. The circles are the experimental data, and the solid line shows the linear fitting of the experimental data.

As observed, the center frequency of the filtered chirped waveform is shifted from about 2.0 GHz to 4.0 GHz when an increased strain is applied. By monitoring the center frequency of the filtered chirped waveform, the applied strain can be measured. However, due to the 200 MHz bandwidth of the MPF, the resolution will be low by simply monitoring the center frequency. A solution to increase the interrogation resolution is to compress the filtered chirped waveform and to measure the temporal location of the compressed pulse. Figure 5(b) shows five filtered chirped waveforms corresponding to the five strains given in Fig. 5(a). The temporal full-width half-maximum (TFWHM) of the chirped waveforms is measured to be 70 ns, which is large, and a direct measurement of the locations of the temporal waveforms may lead to poor resolution. Here, we allow the filtered chirped waveform to correlate with a reference waveform, which is the input chirped waveform, in a DSP. Figure 6(a) shows the correlation outputs corresponding to the five filtered chirped microwave waveforms. As observed, the waveforms are significantly compressed. The TFWHM of the correlation peak is 1 ns. The locations of the five correlation peaks indicate five different wavelength shifts of the PS-FBG. Figure 6(b) shows the correlation peak position vs. the applied strain. As observed, the peak position has a linear relationship with the applied strain. The sensitivity is estimated by linearly fitting the measurements in Fig. 6(b), which is

1.25 ns/µε. Considering the TFWHM of the correlation peak, the interrogation resolution in the experiment is 0.8 µε.

It is known the compressed pulse width depends on the bandwidth of the chirped waveform [10]. A wider bandwidth corresponds to a higher pulse compression ratio. In the experiment, the bandwidth of the filtered chirped waveform is determined by the bandwidth of the MPF. By increasing the MPF bandwidth, a higher pulse compression ratio with an improved resolution can be achieved. In addition, the interrogation speed is determined by the repetition rate of the input LCMW. In our experiment, the repetition rate is 1 MHz, which can be higher if a higher speed DSP is used.

In conclusion, we have proposed and experimentally demonstrated a novel technique to achieve high speed and high resolution interrogation of a PS-FBG sensor based on microwave photonic filtering (MPF) and chirped microwave pulse compression. The key to achieving high speed and high resolution sensing is to convert the wavelength change of a PS-FBG to a temporal shift of an output LCMW using a MPF, which can be interrogated by a DSP. Thus, a high speed and high resolution can be realized. The key feature of the proposed system is the temporal compression of the filtered chirped waveform by correlation, thus the interrogation resolution is improved. Because in the experiment the broadband LCMW was generated at a repetition rate of 1 MHz by an AWG, the interrogation at a speed of 1 MHz was achieved with the assistance of a high speed DSP unit. In addition, the whole system shows good stability during the experiment.

REFERENCES

1. B. Culshaw, J. Lightwave Technol. **22**, 39 (2004).
2. A. D. Kersey, M. A. Davis, H. J. Patrick, M. LeBlane, K. P. Koo, C. G. Askins, M. A. Putnam, and E. J. Friebele, J. Lightwave Technol. **15**, 1442 (1997).
3. Q. Zhang, D. A. Brown, H. Kung, J. E. Townsend, M. Chen, L. J. Reinhart, and T. F. Morse, Electron. Lett. **31**, 480 (1995).
4. H. Xia, C. Zhang, H. Mu, and D. Sun, Appl. Opt. **48**, 189 (2009).
5. A. D. Kersey and T. A. Berkoff, IEEE Photon. Technol. Lett. **4**, 1183 (1992).
6. Y. Rao, Meas. Sci. Technol. **8**, 355 (1997).
7. J. P. Yao, Fiber Integr. Opt. **34**, 204 (2015).
8. H. Fu, W. Zhang, C. Mou, X. Shu, L. Zhang, S. He, and I. Bennion, IEEE Photon. Technol. Lett. **21**, 519 (2009).
9. C. Wang and J. P. Yao, J. Lightwave Technol. **27**, 3336 (2009).
10. W. Liu, M. Li, C. Wang, and J. P. Yao, J. Lightwave Technol. **29**, 1239 (2011).
11. F. Kong, W. Li, and J. P. Yao, Opt. Lett. **38**, 2611 (2013).
12. A. L. Ricchiuti, D. Barrera, S. Sales, L. Thevenaz, and J. Capmany, IEEE Photon. Technol. Lett. **26**, 2039 (2014).
13. Y. P. Wang, J. J. Zhang, O. Coutinho, and J. P. Yao, Opt. Lett. **40**, 4923 (2015).
14. W. Li, M. Li, and J. P. Yao, IEEE Trans. Microw. Theory Technol. **60**, 1287 (2012).